

Scaling and extended scaling in sediment registers of a paleolake perturbed by volcanic activity

Edgardo Ugalde^{a,*}, Gustavo Martínez-Mekler^b, Gloria Vilaclara^c

^a*Instituto de Física, UASLP, Alvaro Obregón 64, 78000 San Luis Potosí, México*

^b*Centro de Ciencias Físicas, UNAM, Apartado Postal 48-3, 62251 Cuernavaca, México*

^c*Facultad de Estudios Superiores, Iztacala, UNAM, Ap. Postal 314, 54090 Tlalnepantla, Mex., México*

Received 5 July 2005; received in revised form 29 September 2005

Available online 5 December 2005

Abstract

We analyze a sequence of density variations of sedimentary material from an extinct paleolake of the state of Tlaxcala, Mexico, which we previously obtained by means of computer-aided tomography [J. Miranda, A. Oliver, G. Vilaclara, R. Rico-Montiel, V.M. Macias, J.L. Ruvalcava, M.A. Zenteno, Nucl. Instrum. Methods Phys. Res. B 85 (1994) 886]. In the stratified blocks chiselled out of mines at the lake bed, low-density sediments have a high concentration of diatomite, while high-density strata show a considerable amount of material external to the lake, mostly of volcanic origin. Two regions can be distinguished by visual inspection: a darker and older one which we attribute to a strongly externally perturbed regime, and a whiter more recent one which appears to have been subjected to less frequent volcanic perturbations. By means of a scaling analysis of the distribution function of density fluctuations, we show that for the most recent region there is a range of scales where these fluctuations present a self-similar behavior. We attribute this observation to a rare event response, namely, the onset of correlations in the lake relaxation processes to steady-state conditions following intense volcanic disturbances. Based on scaling properties of the structure function, we also show that the complete data series presents extended self-similarity as encountered in turbulence studies [R. Benzi, S. Ciliberto, R. Tripicciono, C. Baudet, F. Massoli, S. Succi, Phys. Rev. E 48 (1993) R29]. Our characterization of the statistical behavior of the density fluctuations contributes to our knowledge of the volcanic activity over a period of thousands of years, as well as aspects of ecological interest of the lake's response to these disturbances [G. Vilaclara, E. Ugalde, E. Cuna, G. Martínez-Mekler, Complex dynamics of the evolution of a Paleolake subjected to volcanic activity: geology meets ecology, submitted for publication]. Our approach can be implemented in general to other situations where a scaling characterization may be of interest.

© 2005 Elsevier B.V. All rights reserved.

Keywords: Self-similarity; Lacustrine sediments; Ecology

1. Introduction

Self-similarity and extended self-similarity reflect aspects of the internal organization of a phenomenon. In fluid mechanics, these properties are related to the mechanism of energy transfer from larger to smaller scales

*Corresponding author.

E-mail addresses: ugalde@ifisica.uaslp.mx (E. Ugalde), mekler@fis.unam.mx (G. Martínez-Mekler), amatrin@servidor.unam.mx (G. Vilaclara).



Fig. 1. Section of the Santa Barbara mine from which sediments were extracted. The height of the column is about 2 m.

[1,2]. This kind of behavior has been observed in different natural and social phenomena [3–8]. In this work we analyze the fluctuations of a sequence of computed tomography (CT) X-ray attenuation measurements of sedimentary material extracted from a diatomite mine, dug out at the bed of a paleolake in the state of Tlaxcala, Mexico. We shall in the following indiscriminately use the term density instead of X-ray attenuation since we have shown [9] that both measurements are related via an affine transformation, however, we should stress that the data refer specifically to X-ray attenuation values. These sediments appear stratified in the mine (see Fig. 1) with dark dense strata mainly constituted by volcanic material, and whitish material by diatomite valves (shells). Since the geometry of the valves leaves empty spaces, the density of the sedimentary material is negatively correlated to the algae population. The CT measurements were performed every 0.25 mm. The analyzed data are a measure of the fluctuations of the algae population in the lake, subjected to external perturbations, mainly of volcanic origin.¹ The data series shows two distinguishable regions, the first, older one, more frequently perturbed. The more recent, less perturbed region, presents an asymmetry in the density variations, namely, the increments and decrements follow different statistics. We show that for this region there is a range of scales for which these variations exhibit self-similarity. We argue that this behavior appears as a response to the high-intensity perturbations during relaxation to steady-state conditions. This scaling may hence constitute a signature of the reorganization of the lake system after strong rare events. The above is not the case for the more frequently perturbed older region, where neither asymmetry, nor self-similarity are observed. If these perturbations are too frequent, the lake is unable to relax. Though scaling holds only for part of the data, our extended scaling analysis, which is based on the relation amongst the structure functions of the series, is indicative of the presence of correlations for all the data, including the older, more frequently perturbed region. We have shown elsewhere [10,11] that these differences in the statistical behavior of the perturbed system had an effect in the diatom ecological succession of the lake.

Our study focusses on qualitative aspects of the statistics of the fluctuations. The two main contributions to the paleolake sediments are volcanic ash and diatom depositions, big increments in the density fluctuations result from strong volcanic activity while steady-state conditions are related to the diatom valve deposition disturbed by small volcanic and environmental changes. In the next section, after the data presentation, taking into consideration the two sedimentation processes, we characterize the asymmetry between the increase to and decrease from peak values, performing a rare event scale invariance calculation related to big volcanic disturbances. Further on we calculate the structure functions for positive and negative variations and obtain a scaling exponent consistent with the rare event determination. We then explore the presence of correlations in

¹A detailed geometrical and chemical analysis of the strongest perturbations (highest density) suggests that they are registers of volcanic eruptions.

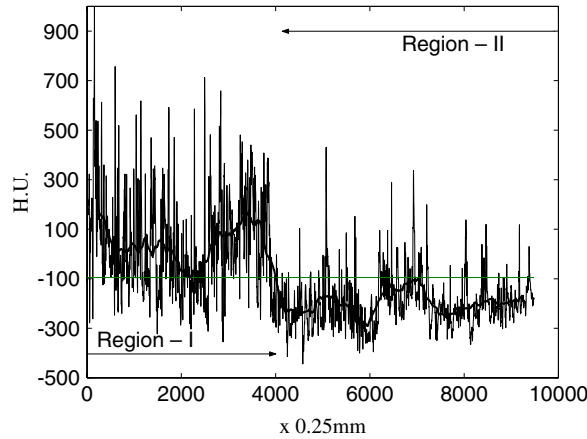


Fig. 2. Computed tomography X-ray attenuation sequence in Hounsfield Units. The horizontal line marks the threshold between the high and low-density regions. The black curve is the moving average of the density, in a window of length 450.

the whole data set by means of an extended scaling calculation. In the final section we sum up and discuss our results. We have also included an Appendix in which we present a general stochastic process formalism on which our scaling and extended scaling calculations are based.

2. Analysis of self-similarity

As mentioned in the Introduction, the series is composed of two regions distinguishable at first sight. The older one has a higher content of dense material, whose mean value of X-ray attenuation is above -100 HU (Hounsfield Units, 0 HU corresponds to water density and -1000 HU to air density).² We shall refer to material with density below this threshold value as rich in diatoms. The recent region of the data series has a moving average below this threshold (see Fig. 2). Based on this criteria we can separate both regions: an older region (Region-I) of length 4010, and a more recent region³ (Region-II) of length $N = 5475$. In the following we shall statistically differentiate these regions keeping in mind that such a characterization may be of use for ecological considerations [10].

Extreme value scaling: As a starting point of our statistical characterization of the processes involved in the lake sedimentation we perform an extreme value calculation for the differences in the density fluctuations at different scales, analyzing separately regions II and I. We first determine the variations of the data values $\{x_n\}$ of Region II at a distance s : $\Delta_s x_n = x_{n+s} - x_n$ and then compute the extrema of these variations defined as

$$\begin{aligned} \max \Delta_s &:= \max\{\Delta_s x_n : n = 1, \dots, N - s\}, \\ \min \Delta_s &:= \min\{\Delta_s x_n : n = 1, \dots, N - s\}, \end{aligned}$$

where N is the number of data being considered. In Fig. 3 we plot these extrema in a log–log scale.

In the interval $[10, 100]$ the $\min \Delta_s$ seem to fluctuate about a linear trend, this behavior is not so apparent for $\max \Delta_s$, where the values decorrelate. This trend can be appreciated better if we look into the behavior of the effective extrema of the variations where we have deleted η fraction of the highest and lowest values of Δ_s :

$$\begin{aligned} \max \Delta_s(\eta) &:= \min \left\{ k : \frac{\#\{n \leq N - s : \Delta_s x_n \geq k\}}{N - s} \leq \eta \right\}, \\ \min \Delta_s(\eta) &:= \max \left\{ k : \frac{\#\{n \leq N - s : \Delta_s x_n \leq k\}}{N - s} \leq \eta \right\}. \end{aligned}$$

²For the sediments we are studying we have determined experimentally that there is an affine transformation between HU and g/cm^3 [9].

³Two peaks were deleted from the original data because their appearance does not conform with the rest of the material and given their dimensions they mask any statistical analysis. These events are however of ecological importance [9,10].

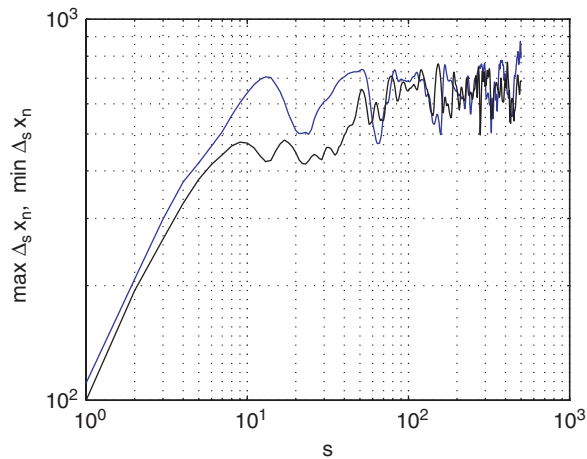


Fig. 3. Log–log plot of the extrema of the X-ray attenuation variations as a function of the scale s for the recent region of the data. The darker line is the absolute value of minima, while the lighter line shows the maxima variations.

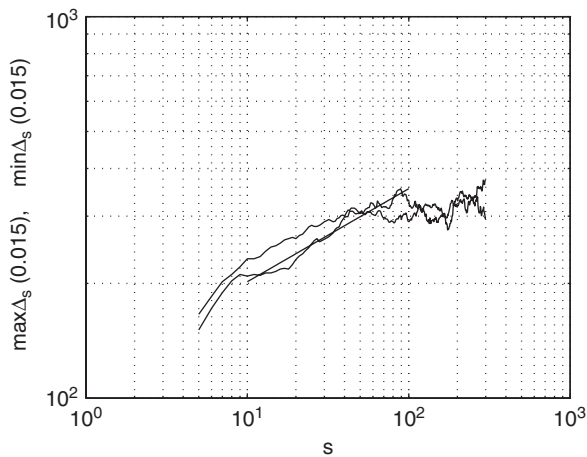


Fig. 4. Log–log plot of η -effective extrema with of the X-ray attenuation variations. The darker curve is the absolute value of the minima, which we compare to a power-law (straight line) in the range $10 \leq s \leq 100$, for $\eta = 0.015$. The lighter line shows the effective maxima.

Fig. 4 suggests a power-law behavior for $\min \Delta_s(\eta)$ in the range $10 \leq s \leq 100$, for $\eta = 0.015$. This appears not to be the case for $\max \Delta_s(\eta)$. In the range $10 \leq s \leq 100$ we can approximate $\min \Delta_s(\eta)$ by a power-law with exponent $\alpha = 0.24 \pm 0.014$.

The previous analysis suggests that the negative tail of the variation distributions shows self-similarity in a range $10 \leq s \leq 100$, with exponent close to $\alpha = 0.24$. In the following section, we argue that this behavior extends to all of the negative variation distributions.

Fig. 5 shows plots for the data of the older region corresponding to Figs. 3 and 4. These graphs show that for the older region one cannot define a self-similarity range.

Structure function scaling: Prompted by the asymmetry we detected in the analysis of the effective extrema, we split the distribution of variations into negative and positive parts and proceed to calculate separately the corresponding structure functions. For the recent region of the series, $\{x_n\}_{n=1}^N$, these are determined from the

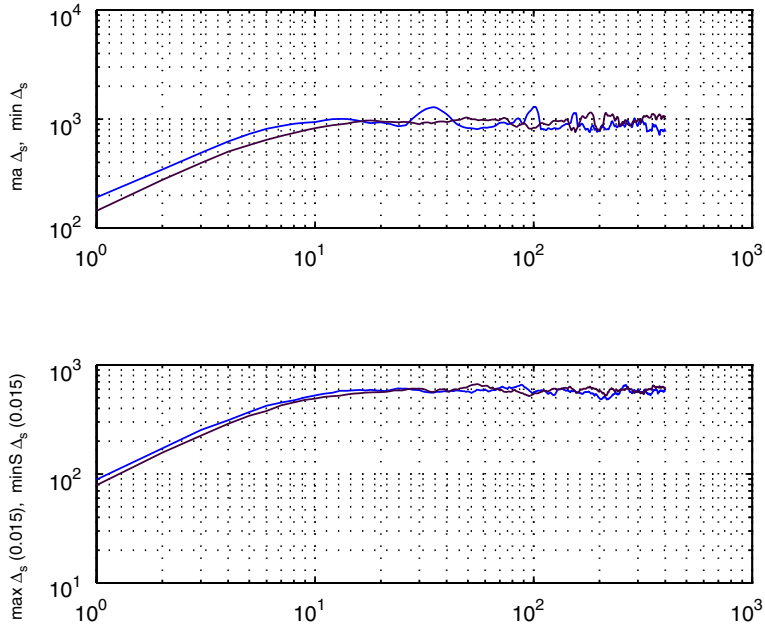


Fig. 5. Log–log plot of the extrema (top) and η -effective extrema with $\eta = 0.015$ (bottom) of the X-ray attenuation variations as a function of the scale s for data’s Region-I. The darker curves are the absolute value of the minima, the lighter lines show the maxima.

following expressions:

$$S_q^+(s) := \frac{\sum_{n=1}^{N-s} ([\Delta_s x_n]^+)^q}{N^+(s)},$$

$$S_q^-(s) := \frac{\sum_{n=1}^{N-s} ([\Delta_s x_n]^-)^q}{N^-(s)},$$

with $[x]^+ := \max(x, 0)$, $[x]^- := [x]^+ - x$, $N^+(s) := \#\{n \leq N - s : \Delta_s x_n \geq 0\}$, and $N^-(s) = N - (N^+(s) + s)$. The overall structure function can be obtained as the addition or the difference of S_q^+ and S_q^- , depending on the parity of q .

Fig. 6 shows the log–log plot of the first six structure functions, for both the negative and positive part of the variation distributions. Since we intend to explore if the scaling observed for the extrema of the negative variations carries on to the whole set of negative variations, we start by assuming scale invariance for the negative structure function for s in the range $10 \leq s \leq 100$. We then proceed with the calculation of the linear regression slopes $\chi^-(q)$, within this range, for the curves of in Fig. 6, namely:

$$\chi^-(q) = \frac{(\bar{n} - \underline{n})(\sum_{s=\underline{n}}^{\bar{n}} \log(s) \log(S_q^-(s))) - (\sum_{s=\underline{n}}^{\bar{n}} \log(s))(\sum_{s=\underline{n}}^{\bar{n}} \log(S_q^-(s)))}{(\bar{n} - \underline{n})(\sum_{s=\underline{n}}^{\bar{n}} \log(s)^2) - (\sum_{s=\underline{n}}^{\bar{n}} \log(s))^2}, \tag{1}$$

with $\underline{n} = 10$ and $\bar{n} = 100$. We then plot these values in Fig. 7 and by performing a linear regression we obtain a power-law for the negative variation structure functions in the range $10 \leq s \leq 100$:

$$S_q^-(s) \approx C_q s^{\alpha^* q}. \tag{2}$$

In the Appendix we show that if a data set satisfies scaling, then α and α^* should coincide. In our case $\alpha = 0.24 \pm 0.01 \approx \alpha^* = 0.26 \pm 0.03$ provides a consistency test that gives support to our scaling assumption.

Though the positive extrema do not show a power-law behavior we perform the same calculation as above for the structure functions S_q^+ . In this case a linear regression calculation is meaningless given the size of the uncertainties (see lower part of Fig. 7).

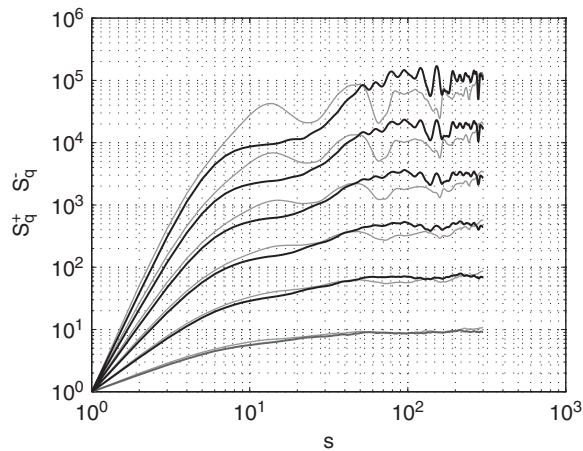


Fig. 6. The negative (solid bold curves) and positive structure functions (gray lines) S_q^- and S_q^+ as a function of s in a log–log scale, for $q = 1–6$. The curves have been vertically shifted so that they coincide at $s = 1$.

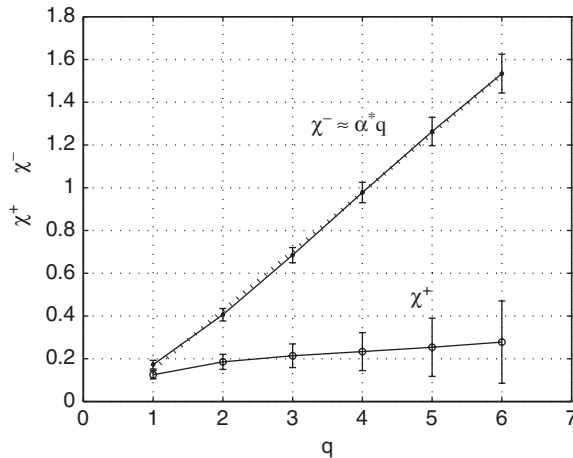


Fig. 7. The higher curve joining the circles shows the exponent law $\chi^-(q)$ for the negative structure functions, which is in good agreement with the linear regression dotted line with slope $\alpha^* = 0.26 \pm 0.03$. The lower curve corresponds to $\chi^+(q)$ computed from the positive structure functions. Note the differences in the error bars of both curves.

Despite structure function scaling does not hold neither in the positive fluctuations of the recent part of the series, nor in the positive or negative fluctuations of the old region of the series, there is a correlation amongst the scales which is present in the whole series which involves both positive and negative fluctuations. This correlation becomes apparent through the extended self-similarity determination shown below.

Extended self-similarity: The formal definition and significance of extended scaling is presented in the Appendix. It relates to nonhomogeneous scale invariance properties of the data. The main consequence of extended self-similarity is that the data structure functions are interrelated in terms of power laws, e.g., $S_q \propto (S_2)^{q/2}$ for all q (see Appendix Eq. (8)). To test for extended self-similarity we compute the structure functions

$$S_q(s) := \frac{\sum_{n=1}^{N-s} |A_s x_n|^q}{N-s},$$

including positive and negative variations, considering both Region-I and Region-II, and plot them in a log–log scale in Fig. 8 as functions of S_2 . Note the straight line behavior for all S_q required by extended

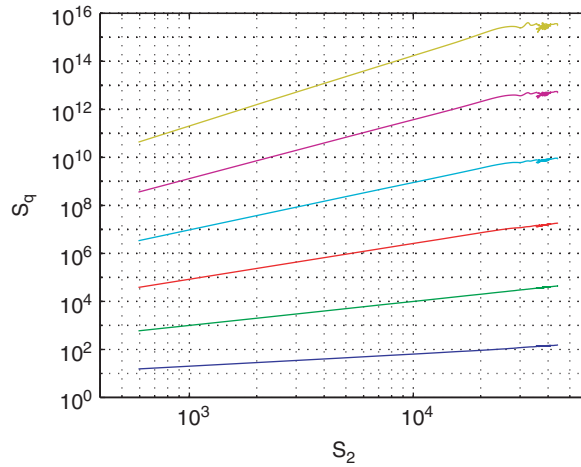


Fig. 8. Log–log plot of the structure functions S_q of the whole data series versus the second structure function S_2 , for $q = 1–6$.

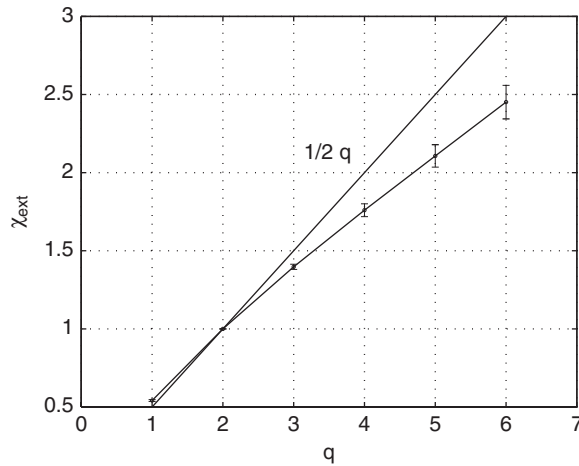


Fig. 9. The straight line is the expected linear law for the exponents associated to extended self-similarity. The curve below it is the actual exponent law with its corresponding error bars.

self-similarity. From Fig. 8 we can determine

$$S_q \propto (S_2)^{\chi_{\text{ext}}(q)},$$

where $\chi_{\text{ext}}(q)$ is defined as in (1) substituting s by S_2 and considering the structure function for the whole series. As mentioned above, for large N , extended self-similarity predicts $\chi_{\text{ext}}(q) = q/2$. In Fig. 9 we show a deviation from this linear dependence of the exponents. The type of concave, increasingly larger deviation, from the asymptotic behavior has been shown to be expected due to finite size effects. Higher order structure functions require larger amounts of data in order to attain the asymptotic regime (see Ref. [12] for an explanation). Taking this into account, our whole data supports extended self-similarity.

3. Conclusions and final remarks

In this work we have presented a statistical study of fluctuating phenomena with scale invariance that has been subjected to external perturbations. By exhibiting the asymmetry in the fluctuations we have been able to

characterize “charging” and “relaxation processes”. We have associated a scaling regime with the systems response to strong perturbations. During the relaxation from rare events the ensuing scale invariance might be interpreted as a signature of the presence of underlying organization processes.

Our study singles out two regions: one highly perturbed the other less perturbed. In the first one, the perturbation characteristic times are shorter than the systems’ response times, precluding the onset of relaxation dynamics.

We have shown that extended scaling holds for the whole data series. This is an indication of the presence of correlations among all scales which are robust under external perturbations. Extended scaling always holds when there is scaling. We corroborated, based on consistency arguments, that this relation holds for the relaxation processes of the less perturbed region which show scaling.

A special feature of our work is that we are dealing with field data of ecological significance. In this respect our findings have been useful to determine properties of the lacustrine evolution of an extinct paleolake, giving insight related amongst others to the self-organization and succession of its population [10].

We should point out the qualitative nature of our analysis which is mainly concerned with the detection of scale-dependent properties. Once these have been identified we assume plausible scaling behaviors that we then validate through consistency tests. Our approach can be implemented for the study of a variety of relatively small data series.

Acknowledgements

This work was supported by CONACyT through Grants J32389-E and 34512-E, and by the ECOS-ANUIES program through Grant M04-M01. E.U. and G.M.-M. thank the CPT-CNRS Luminy hospitality.

Appendix

Self-similarity and its indicators: Consider a stationary process x_0, x_1, \dots taking values in \mathbb{R} , with probability distribution \mathbb{P} . For each $s, n \in \mathbb{N}$ define the variation $\Delta_s x_n := x_{n+s} - x_n$. We say that the process $\{x_n\}_{n \in \mathbb{N}}$ is self-similar with respect to the variations in the range $[\underline{\lambda}, \bar{\lambda}]$, if there exists $\alpha > 0$ such that, for any $s \in [\underline{\lambda}, \bar{\lambda}]$ and $\lambda > 0$, with $\lambda s \in [\underline{\lambda}, \bar{\lambda}]$, we have

$$\mathbb{P}\{\Delta_s x_n \in [a, b]\} = \mathbb{P}\{\Delta_{\lambda s} x_n \in [\lambda^\alpha a, \lambda^\alpha b]\}, \quad (3)$$

for every interval $[a, b] \subset \mathbb{R}$. Alternatively, we can associate to each scale $s \in [\underline{\lambda}, \bar{\lambda}]$ a probability density function ρ_s , such that

$$\mathbb{P}\{\Delta_s x_n \in [a, b]\} = \int_a^b \rho_s(\xi) d\xi.$$

Here, we assume that the distributions involved are absolutely continuous. In this case, self-similarity is equivalent to

$$\rho_s(\xi) = \lambda^\alpha \rho_{\lambda s}(\lambda^\alpha \xi),$$

for any $s \in [\underline{\lambda}, \bar{\lambda}]$ and $\lambda > 0$ such that $\lambda s \in [\underline{\lambda}, \bar{\lambda}]$.

The size s of the variation may be thought of as an observation scale, thus, self-similarity means that observations at different scales are statistically equivalent after a suitable homogeneous change of scale in the observed variable. This situation holds inside a range of scales $[\underline{\lambda}, \bar{\lambda}]$.

We will assume in the following that, for each observation scale, the distribution function $F_s(\xi) := \mathbb{P}\{\Delta_s x_n \leq \xi\}$ is strictly increasing. Furthermore, we shall also assume that the process x_0, x_1, \dots which we are observing is ergodic, which in our present case means that the spatial statistics⁴ of a typical realization reproduces the distribution of the process.

⁴Usually one refers to temporal statistics, however, our X-ray attenuation data are space dependent, and even though there is a monotonous increasing relation between spatial measurements and time, the functional form is not determined. For instance, rich volcanic sediments accumulate at a much faster rate than diatom-rich sediments.

Indicators of self-similarity: We define the η -effective extrema of the variations, for $\eta \in (0, 1)$ by

$$\begin{aligned} \max \Delta_s(\eta) &:= \min\{\xi \in \mathbb{R} : \mathbb{P}\{\Delta_s x_n \geq \xi\} \leq \eta\}, \\ \min \Delta_s(\eta) &:= \max\{\xi \in \mathbb{R} : \mathbb{P}\{\Delta_s x_n \leq \xi\} \leq \eta\}. \end{aligned} \tag{4}$$

They will occur with a prescribed positive probability, and under the assumption that the distribution function F_s are strictly increasing, more extreme variations are less probable. Self-similarity may then be observed through the behavior of the effective extrema. For η fixed, if the process $\{x_n\}_{n \in \mathbb{N}}$ is self-similar in the range $[\underline{n}, \bar{n}]$, then

$$\begin{aligned} \max \Delta_{\lambda s}(\eta) &= \lambda^\alpha \max \Delta_s(\eta), \\ \min \Delta_{\lambda s}(\eta) &= \lambda^\alpha \min \Delta_s(\eta), \end{aligned} \tag{5}$$

for any $s \in [\underline{n}, \bar{n}]$ and $\lambda > 0$ such that $\lambda s \in [\underline{n}, \bar{n}]$. These relations can be deduced directly from Eq. (3).⁵

Another important consequence of self-similarity is a power-law behavior of the structure functions defined by

$$s \mapsto S_q(s) := \mathbb{E}(|\Delta_s x_n|^q)$$

for each $q \in \mathbb{N}$, where $\mathbb{E}(X)$ denotes the expectation of the random variable X with respect to \mathbb{P} . Due to self-similarity,

$$S_q(\lambda s) = \lambda^{q\alpha} S_q(s), \tag{6}$$

for $s \in [\underline{n}, \bar{n}]$ and $\lambda > 0$ such that $\lambda s \in [\underline{n}, \bar{n}]$. One of the earliest derivations of this fact can be found in Ref. [13]. Note that this power-law behavior is valid only in the range where self-similarity holds, which may be small compared to the total length of the fluctuation record.

Thus, in order to detect and quantify self-similarity, we compute the effective extrema and structure functions, and look for an interval $[\underline{n}, \bar{n}]$ where these quantities follow a power-law behavior. If such an interval exists and the corresponding exponents are integer multiples of some number $\alpha \in \mathbb{R}$, we consider the process as self-similar. Though these are strictly necessary conditions, under very general assumptions there also sufficient conditions.⁶

The power spectrum of the series is related to the second structure function ($q = 2$) via a Fourier transform, therefore, it inherits a power-law behavior from the later.⁷ However, the power spectrum involves the whole range of scales, and hence contributions from outside the self-similarity range may alter the power-law behavior. Since in our case the self-similarity range is small compared to the whole range of scales, it is preferable to use structure functions as indicators of self-similarity. An interesting remark is that the log–log plot of the power spectrum [10] shows two linear trends, one of which (long wave length regime) coincides with the self-similarity here reported. This type of behavior of the power spectrum has been encountered in other externally perturbed systems [8].

Extended self-similarity: Suppose that for any $s, s' \in [\underline{n}, \bar{n}]$, the distributions $F_s(\xi)$ and $F_{s'}(\xi)$ can be collapsed onto a single distribution after a suitable change of scales. Under this assumption, whenever self-similarity holds, the change of scales we need is given by a simple power-law of the scale of observation, i.e. if we change the scale of observation $s \rightarrow \lambda s$, then the observed quantity has to be rescaled as $\xi \rightarrow \lambda^\alpha \xi$. A weaker version of self-similarity occurs if the rescaling of the observed quantity follows a more complicated rule, which may depend on the two scales of observation we want to compare, namely s and $s' = \lambda s$. In this case we have a non-homogeneous change of scales.

We say that the process $\{x_n\}_{n \in \mathbb{N}}$ has extended self-similarity in the range $[\underline{n}, \bar{n}]$, with gauge function $g : [\underline{n}, \bar{n}] \rightarrow \mathbb{R}^+$, if for each $s, s' \in [\underline{n}, \bar{n}]$ and $a < b$,

$$\mathbb{P}\{\Delta_s x_n \in [a, b]\} = \mathbb{P}\left\{\Delta_{s'} x_n \in \frac{g(s')}{g(s)} [a, b]\right\}. \tag{7}$$

⁵See Ref. [12] for details.

⁶See Ref. [14, p. 267] for details.

⁷See Ref. [15] for details.

Alternatively, extended self-similarity can be expressed by requiring that the probability density function ρ_s associated to each scale $s \in [\underline{n}, \bar{n}]$ satisfy

$$\rho_s(\xi) = \frac{g(s')}{g(s)} \rho_{s'}\left(\frac{g(s')}{g(s)} \xi\right),$$

for any $s, s' \in [\underline{n}, \bar{n}]$. The gauge function gives the rescaling rule $\xi \rightarrow g(s')/g(s) \times \xi$ required by the change of the observation scale $s \rightarrow s'$. In this case we cannot attach a single exponent to the extended self-similarity as we did in the case of self-similarity.

An important consequence of the extended self-similarity is that the q structure functions follow power laws as functions of a fixed structure function. This was in fact the definition of extended self-similarity first introduced by Benzi et al. in Ref. [16], where they took the second structure function as reference. To be more precise, if the process $\{x_n\}_{n \in \mathbb{N}}$ has extended self-similarity in the range $[\underline{n}, \bar{n}]$, then for any $s, s_0 \in [\underline{n}, \bar{n}]$ and $q \in \mathbb{N}$ we have $S_q(s) = (g(s)/g(s_0))^q S_q(s_0)$. Hence, for any fixed $q_0 \in \mathbb{N}$ we obtain

$$S_q(s) = \left(\frac{S_q(s_0)}{S_{q_0}(s_0)^{q/q_0}} \right) \times S_{q_0}(s)^{q/q_0}, \quad (8)$$

for every s in the range $[\underline{n}, \bar{n}]$ of extended self-similarity. Thus, if self-similarity holds in the whole range of observation scales, then $S_q \propto (S_{q_0})^{q/q_0}$ for any $q, q_0 \in \mathbb{N}$. Therefore, an indicator of extended self-similarity is the power-law dependence of the structure functions when considered as functions of a fixed structure function.

General remark: We are assuming an ergodic hypothesis under which the quantities defined in this Appendix correspond to the asymptotic values of their finite N counterparts calculated in the main text.

References

- [1] G. Paladin, A. Vulpiani, Phys. Reports 156 (4) (1987) 147.
- [2] E. Aurell, U. Frisch, J. Lustko, M. Vergassola, J. Fluid Mech. 238 (1992) 467.
- [3] P.G. De Gennes, Scaling Concepts in Polymer Physics, Cornell University Press, 1979.
- [4] J. Rundle, D.L. Turcotte, W. Klein, Geocomplexity in the Physics of Earthquakes, American Geophysical Union, 2000.
- [5] S. Drożdż, F. Ruf, J. Speth, M. Wójcik, Eur. Phys. J. B 10 (1999) 589.
- [6] R. Solé, S.C. Manrubia, M. Benton, P. Bak, Nature 388 (1997) 764.
- [7] D.H. Zanette, Adv. Complex Systems 4 (2–3) (2001) 281.
- [8] V. Uritsky, M. Pudovkin, A. Steen, J. Atmos. Solar–Terrestrial Phys. 63 (2001) 1415.
- [9] G. Vilaclara, J. Miranda, E. Cuna, G. Martinez-Mekler, Characterization of small scale fluctuations in lacustrine sediments using X-ray computed tomography, submitted for publication.
- [10] G. Vilaclara, E. Ugalde, E. Cuna, G. Martinez-Mekler, Complex dynamics of the evolution of a paleolake subjected to volcanic activity: geology meets ecology, submitted for publication.
- [11] G. Vilaclara, E. Cuna, G. Martinez-Mekler, Diatom-inferred environment of a paleolake disturbed by volcanic activity in Central Mexico, submitted for publication.
- [12] E. Ugalde, J. Phys. A 29 (1996) 4425.
- [13] C.W. Van Atta, J. Park, in: Statistical Models and Turbulence, Lecture Notes in Physics, vol. 12, 1972, p. 402.
- [14] W. Feller, An Introduction to Probability Theory and its Applications, vol. II, Wiley, New York.
- [15] U. Frisch, Turbulence: The Legacy of A.N. Kolmogorov, Cambridge University Press, Cambridge, 1995.
- [16] R. Benzi, S. Ciliberto, R. Tripiccone, C. Baudet, F. Massoli, S. Succi, Phys. Rev. E 48 (1993) R29.